

This is the accepted manuscript made available via CHORUS. The article has been published as:

Signature inversion in odd-odd ^{114}Rh : First
identification of high-spin states in very neutron-rich
 ^{114}Rh and application of the triaxial projected shell
model

S. H. Liu, J. H. Hamilton, A. V. Ramayya, Y. S. Chen, Z. C. Gao, S. J. Zhu, L. Gu, E. Y. Yeoh,
N. T. Brewer, J. K. Hwang, Y. X. Luo, J. O. Rasmussen, W. C. Ma, J. C. Batchelder, A. V.
Daniel, G. M. Ter-Akopian, Yu. Ts. Oganessian, and A. Gelberg

Phys. Rev. C **83**, 064310 — Published 13 June 2011

DOI: [10.1103/PhysRevC.83.064310](https://doi.org/10.1103/PhysRevC.83.064310)

Signature inversion in odd-odd ^{114}Rh : first identification of high-spin states in very neutron-rich ^{114}Rh and application of the triaxial projected shell model

S. H. Liu,^{1,2} J. H. Hamilton,¹ A. V. Ramayya,¹ Y. S. Chen,³ Z. C. Gao,³ S. J. Zhu,⁴ L. Gu,⁴ E. Y. Yeoh,⁴ N. T. Brewer,¹ J. K. Hwang,¹ Y. X. Luo,^{1,5} J. O. Rasmussen,⁵ W. C. Ma,⁶ J. C. Batchelder,² A. V. Daniel,^{1,7} G. M. Ter-Akopian,⁷ Yu. Ts. Oganessian,⁷ and A. Gelberg⁸

¹*Department of Physics and Astronomy, Vanderbilt University, Nashville, Tennessee 37235, USA*

²*UNIRIB/Oak Ridge Associated Universities, Oak Ridge, Tennessee 37831, USA*

³*China Institute of Atomic Energy, P.O. Box 275(18), Beijing 102413, People's Republic of China*

⁴*Department of Physics, Tsinghua University, Beijing 100084, People's Republic of China*

⁵*Lawrence Berkeley National Laboratory, Berkeley, California 94720, USA*

⁶*Department of Physics and Astronomy, Mississippi State University, Mississippi State, Mississippi 39762, USA*

⁷*Joint Institute for Nuclear Research, RU-141980 Dubna, Russian Federation*

⁸*Institut für Kernphysik, Universität zu Köln, 50937 Cologne, Germany*

High-spin excited states in the very neutron-rich nucleus ^{114}Rh have been studied by examining the prompt γ rays emitted in the spontaneous fission of ^{252}Cf with the Gammasphere detector array. A high-spin level scheme of ^{114}Rh has been established for the first time with thirteen new levels. The level scheme is proposed to be built on a 7^- state. The existence of a relatively large signature splitting and an yrare band show features which may indicate triaxial deformation. The phenomenon of signature inversion has been observed in ^{114}Rh at $I = 12\hbar$. The observed signature inversion of ^{114}Rh is interpreted successfully in terms of the triaxial projected shell model. Theoretical calculations suggest that the negative-parity, yrast band of ^{114}Rh has the two-quasi-particle configuration of $\pi g_{9/2} \otimes \nu h_{11/2}$, consistent with the systematics of odd-odd Rh isotopes. The signature inversion at spin $12\hbar$ may be attributed to the change of rotational mode, from quasi-particle aligned rotation at low spins to collective rotation at high spins.

PACS numbers: 27.60.+j, 23.20.Lv, 21.60.Cs, 25.85.Ca

I. INTRODUCTION

Neutron-rich nuclei in the $A = 110$ region are of great interest because they are characterized by shape coexistence and shape transitions, including triaxial shapes [1–3]. In this region, the active proton orbitals, midway in the $\pi g_{9/2}$ sub-shell, can drive the nuclear shape towards oblate, prolate or triaxial deformations, while the neutron Fermi levels, below or near the bottom of the $\nu h_{11/2}$ sub-shell, drive the shape to prolate or triaxial deformations. These tendencies have been observed in the yrast bands of neighboring odd- A nuclei, which are built on the $\pi g_{9/2}$ and $\nu h_{11/2}$ orbitals. The proton orbitals originating from the $g_{9/2}$ sub-shell are influenced by the triaxial nuclear deformation. The appearance of triaxial deformations and soft shape transitions were found in nuclei of $Z \geq 41$ [3–7].

Odd-odd neutron-rich Rh isotopes are located in this mass region, and a remarkable similarity in their high-spin, negative-parity yrast states is seen throughout a large range of neutron numbers from 59 (^{104}Rh) to 67 (^{112}Rh) [7–10]. Earlier investigations of these Rh isotopes in β -decay studies established their low-lying excited states, where their ground states were found to have a spin-parity of 1^+ [11]. High-spin states of negative parity in odd-odd $^{104-112}\text{Rh}$ have been built based on their positive-parity isomeric states [7–10]. A 6^+ isomeric state was proposed for $^{106,112}\text{Rh}$ while a 5^+ isomeric state was proposed for $^{104,108,110}\text{Rh}$ [7–10]. The band-heads of their negative-parity yrast bands have a spin-parity of 6^-

with a 7^- intermediate state from $N = 59$ to $N = 65$ and then it becomes 7^- at $N = 67$ (^{112}Rh). These $\Delta I = 1$, negative-parity yrast bands originating from the coupling of a proton in the $g_{9/2}$ orbital with a strongly aligned $h_{11/2}$ neutron are present at low and moderate excitations. In addition, the phenomenon of signature inversion in $^{98,100,102}\text{Rh}$ has recently been observed and studied [12–15].

Thus, it is worth exploring the structure of odd-odd Rh isotopes in the more neutron-rich region with $N \geq 69$. Low-lying states in ^{114}Rh ($N = 69$) were observed in β -decay studies [16] where the ground state was determined as 1^+ , following the systematics of odd-odd $^{104-112}\text{Rh}$. A definite odd parity and a probable $I = 7$ were deduced for a high-spin level in ^{114}Rh by studying the β -decay of ^{114}Rh to ^{114}Pd [17]. Here, we establish a high-spin level scheme of ^{114}Rh for the first time along with the observation of signature inversion in its yrast band.

II. EXPERIMENTAL RESULTS

Studies of the spontaneous fission of ^{252}Cf with multi-gamma-detector arrays give a powerful approach for identifications of high-spin states in neutron-rich nuclei [3]. Data for this work were collected by using the Gammasphere detector array at Lawrence Berkeley National Laboratory. A ^{252}Cf spontaneous fission source of 62 μCi was placed between two iron foils of 10 mg/cm^2 , which were used to stop the fission fragments and elimi-

nate the need for a Doppler correction. A plastic ball of 7.62 cm in diameter, surrounding the source, was used to absorb β rays and conversion electrons, as well as to partially moderate and absorb fission neutrons. A total of 5.7×10^{11} triple- and higher-fold γ -ray coincidence events were recorded. Data were analyzed with the RadWare software package [18]. The basic idea to identify new transitions in an unknown nucleus is to gate on transitions in its partner isotopes and compare their fission yields. The fission partners of ^{114}Rh are I isotopes, namely $^{133-136}\text{I}$.

Two spectra were obtained by double-gating on transitions in ^{134}I [19] and ^{135}I [20], respectively, as shown in Fig. 1, where two new transitions of energies 195.9 and 278.1 keV are seen, along with those previously known strong transitions in $^{111,112,113}\text{Rh}$ [7, 9]. The spectra gated on the new 195.9-keV transition and the 952.4-keV transition in ^{134}I as well as the 1133.8-keV transition in ^{135}I show three new transitions of energies 211.2, 264.1, and 297.5 keV, as indicated in Fig. 2 a and b. Shown in Fig. 2 c (d) is the spectrum gated on the new 278.1-keV transition and the 952.4-keV transition in ^{134}I (the 1133.8-keV transition in ^{135}I), where one sees the same new transition of energy 211.2 keV as in Fig. 2 a and b, besides a new 324.5-keV transition. The spectra gated on the new 195.9- and 264.1-keV transitions, the new 195.9- and 211.2-keV transitions, and the new 278.1- and 324.5-keV transitions show the other new transitions, such as the 317.0-, 420.9-, 432.3-, and 318.2-keV transitions, and the coincidence relationships among these new transitions and those known ones in $^{133-136}\text{I}$ [19–22], as shown in Fig. 3. These data enable us to establish a new level scheme belonging to a single Rh isotope, as shown in Fig. 4.

A method, which has been successfully used for our work in ^{134}I [19] and $^{139,140,142}\text{Cs}$ [23] was adopted to determine the mass number of the present level scheme. In the 279.7/224.8- (^{111}Rh), 60.6/183.0- (^{112}Rh), 232.2/240.6- (^{113}Rh), and 195.9/264.1-keV double gates, the fission yield ratios of the 1111.8-keV transition in ^{136}I [22] to the 1133.8-keV transition in ^{135}I [20] were measured to be 0.80(11), 0.55(8), 0.32(4), and 0.21(3), respectively. The variation of these ratios follows those of ^{142}Cs to ^{141}Cs in the $^{105-108}\text{Tc}$ gates, as presented in Fig. 5. So it is reasonable to assign the mass number 114 to the level scheme we established. The spin-parity assignments to the levels in the level scheme of ^{114}Rh as shown in Fig. 4 are mainly based upon the analogy with the level structures of the lighter odd-odd Rh isotopes.

III. DISCUSSION AND CALCULATIONS

The $\Delta I = 1$, negative-parity yrast band assigned to ^{114}Rh as displayed in Fig. 4, together with the level schemes built on the $\pi g_{9/2} \otimes \nu h_{11/2}$ configuration in odd-odd $^{104-112}\text{Rh}$, shows a striking similarity that supports

a common interpretation for all bands, as presented in Fig. 6. Therefore, it is reasonable to propose that the present high-spin level scheme of ^{114}Rh is built on a 7^- state with the $\pi g_{9/2} \otimes \nu h_{11/2}$ configuration, which is solidified by the theoretical calculations presented later. Figure 6 shows the $\Delta I = 1$ level structures of odd-odd $^{104-114}\text{Rh}$ based on a 7^- state in each nucleus. On the basis of this similarity, spins and parities were assigned to the states of the yrast band of ^{114}Rh , as presented in Fig. 4. With the assumption that the 278.1-keV transition has an $E2/M1$ character, spins and parities were assigned to the levels in the side-band in ^{114}Rh except for the 1309.1-keV state.

Note that the 7^- states of these $\Delta I = 1$, negative-parity bands decay either to the 5^+ (or 6^+) isomeric state through a 6^- state in odd-odd $^{104-110}\text{Rh}$ or directly to the 6^+ isomeric state in ^{112}Rh . However, we have not observed any transition depopulating the 7^- state in ^{114}Rh to an isomeric state. Note that in the case of ^{112}Rh the $7^- \rightarrow 6^+$ transition has a small transition energy of 60.6 keV. It is possible that the $7^- \rightarrow 6^+$ transition in ^{114}Rh has a much smaller transition energy than 30 keV, the detection energy cutoff for our experiment. Another possibility is that there is no such a positive isomeric state in ^{114}Rh , as indicated in Ref. [17].

The signature is a quantum number associated with the invariance of a system with an intrinsic quadrupole deformation under a rotation of 180° around a principal axis[25]. Due to this symmetry, level energies $E(I)$ of a high- j rotation band are split into two branches with $\Delta I = 2$, classified by the signature quantum number α . The signature splitting is a measure of the difference of the Routhians (the energy referring to the rotating coordinate system) between the two signature branches of a rotation band. This quantity can be used as an indicator of the shape of a nucleus. Triaxial deformations can contribute to a large signature splitting, because K is not a good quantum number any longer. Also as a rule, the energetically favored signature sequence in an odd-odd nucleus has the signature $\alpha_f = \frac{1}{2} [(-1)^{j_\nu - 1/2} + (-1)^{j_\pi - 1/2}]$ [26], which gives $\alpha_f = 0$ (even-integer spins) to the $\pi g_{9/2} \otimes \nu h_{11/2}$ configuration of ^{114}Rh . If the Routhian of the favored signature is found to lie higher in energy as compared to that of the unfavored one, the corresponding signature splitting is anomalous. The signature splitting becomes normal at some spin where signature inversion occurs.

$E(I) - E(I - 1)$ (energy difference) vs spin is plotted for the yrast band of ^{114}Rh in Fig. 7, which is a simple way to investigate the phenomenon of signature inversion. One clearly sees $E(I) - E(I - 1)$ in the favored signature branch with even-integer spins is located above that in the unfavored signature branch with odd-integer spins at low spins. The energy differences in the favored signature branch are lower than those in the unfavored branch after $I = 12\hbar$, where the signature inversion emerges. After that, the signature splitting becomes normal and the anomalous splitting disappears. The crit-

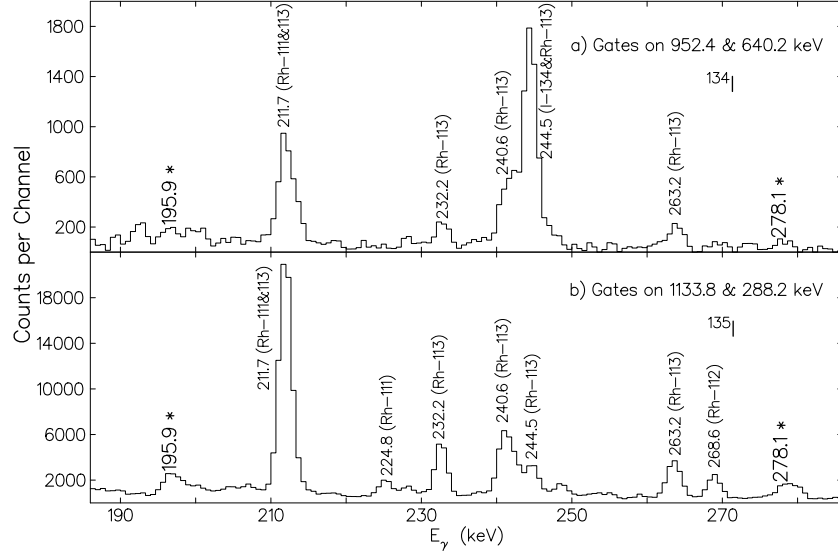


FIG. 1. Coincidence spectra gated on transitions in $^{134,135}\text{I}$. Two new transitions of energies 195.9 and 278.1 keV are indicated with an asterisk.

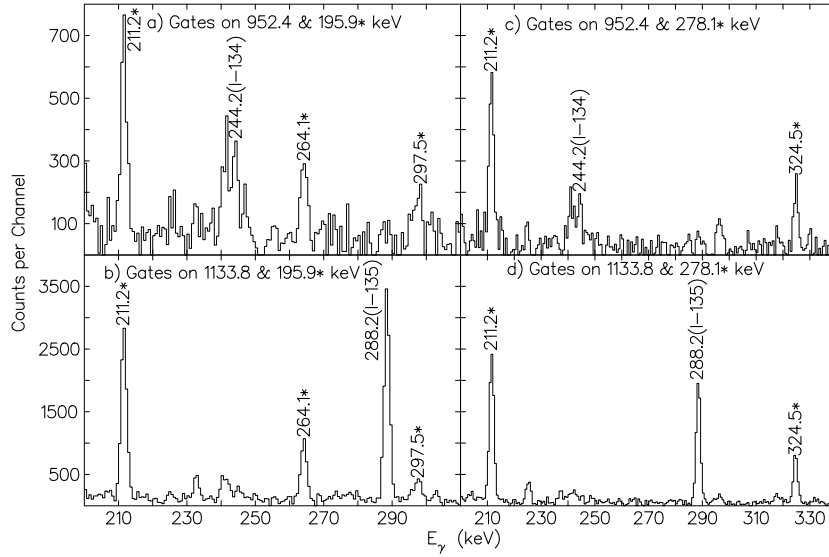


FIG. 2. Coincidence spectra gated on the new 195.9-, 278.1-keV transitions and the 952.4- in ^{134}I , 1133.8-keV in ^{135}I transitions. Four new transitions of energies 211.2, 264.1, 297.5, and 324.5 keV are marked with an asterisk.

ical spin where the signature changes from the abnormal phase to the normal one is called the reversion spin I_{rev} [27]. So $I_{\text{rev}} = 12\hbar$ for ^{114}Rh as shown in Fig. 7. One also sees a significantly larger signature splitting in ^{114}Rh for the states higher than I_{rev} .

The observation of the anomalous signature splitting and the signature inversion is a common feature in many mass regions, $A = 80, 100, 130, 160$. Generally, the normal signature splitting is achieved above a certain spin value, which depends on the nucleon numbers. The

mechanism of signature inversion has been studied in various theoretical frameworks with different explanations. Some of them involve the influence of triaxial shapes. A residual proton-neutron interaction with an axially symmetric core can induce the signature inversion as well. The signature inversion can also be obtained in the projected shell-model framework with axial symmetric shapes resulting from the crossing of different bands with opposite signature dependence [28]. After that, the triaxial projected shell-model in a realistic configuration

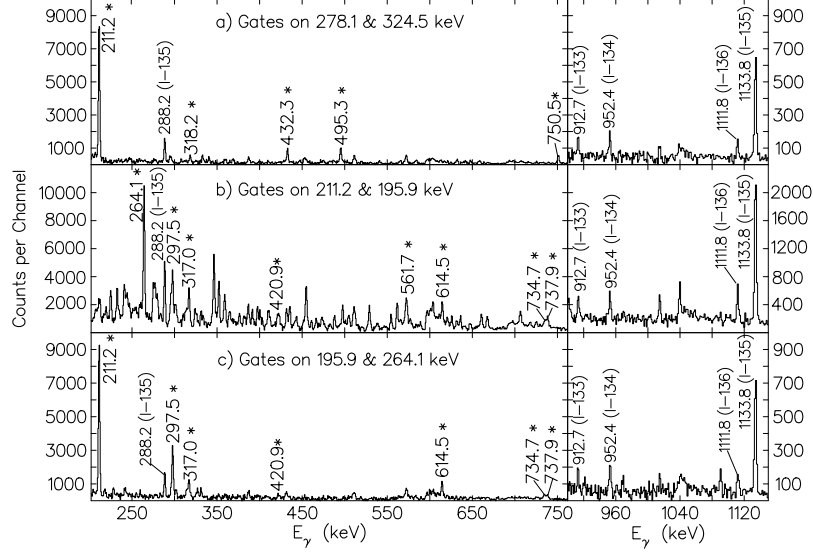


FIG. 3. Coincidence spectra gated on the new 195.9- and 264.1-keV transitions, the new 195.9- and 211.2- keV transitions, and the new 278.1- and 324.5-keV transitions. All newly observed transitions are marked with an asterisk.

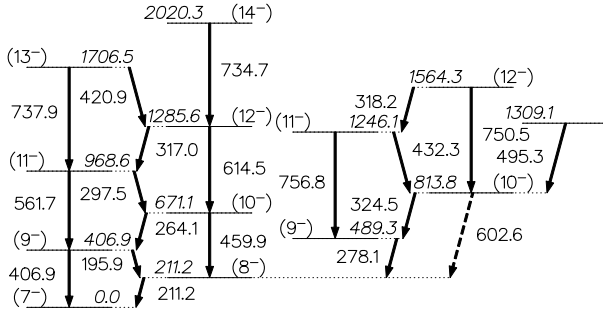


FIG. 4. Partial high-spin level scheme of ^{114}Rh built in the present work. All transitions are newly observed.

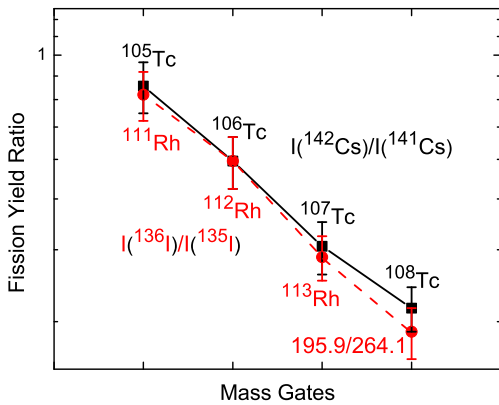


FIG. 5. (Color online) Fission yield ratios of ^{136}I to ^{135}I in Rh gates and those of ^{142}Cs to ^{141}Cs in Tc gates. Data are taken from Refs. [7, 11, 20, 22–24] and the present work. A logarithmic scale is used for the y -axis.

space was developed and used to reproduce the signature inversion in the $A = 130$ region very well [29]. More recently, a few theoretical calculations have been done for the signature inversion observed in $A \approx 100$ Rh and Ag isotopes [12–15].

Regarding ^{114}Rh , it is likely that triaxiality plays an important role in its nuclear structure with its clear signature splitting by spin 12 and a side-band feeding the 8^- state in the yrast band (This side-band is called the yrare band. See Ref. [30]). Therefore, triaxial-projected-shell-model (TPSM) calculations have been performed for ^{114}Rh to study the observed signature inversion. The theory is briefly described below, and more details of the TPSM and its application for a new understanding of the signature inversion phenomenon can be found in Ref.[29]. In the TPSM theory, the wave-function is written as

$$|\Psi_{IM}^\sigma\rangle = \sum_{K\kappa} f_{IK\kappa}^\sigma \hat{P}_{MK}^I |\Phi_\kappa\rangle. \quad (1)$$

In Eq. (1), $|\Phi_\kappa\rangle$ represents a set of two-, four-, and six-quasi-particle (qp) states associated with the triaxially deformed qp vacuum $|0\rangle$ for odd-odd nuclei. The qp states are obtained by carrying out the standard BCS calculation from the triaxially deformed Nilsson single-particle basis states. The shell-model space is then built by establishing multi-quasi-particle states from the deformed Nilsson orbitals which lie close to the Fermi levels. To form the shell-model basis in the laboratory frame, the broken rotational and axial symmetries in the deformed multi-quasi-particle states are necessarily recovered by extracting three dimensional angular-momentum projection, where the projection operator is \hat{P}_{MK}^I . The

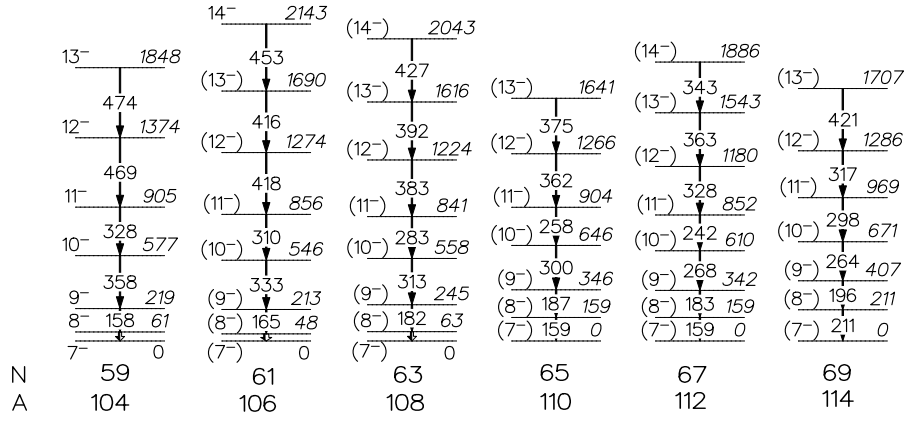


FIG. 6. $\Delta I = 1$, negative-parity yrast bands of odd-odd $^{104-114}\text{Rh}$ associated with the $\pi g_{9/2} \otimes \nu h_{11/2}$ configuration. Level energies are relative to the corresponding 7^- state. Data are taken from the present work for ^{114}Rh and Refs. [7–10] for others.

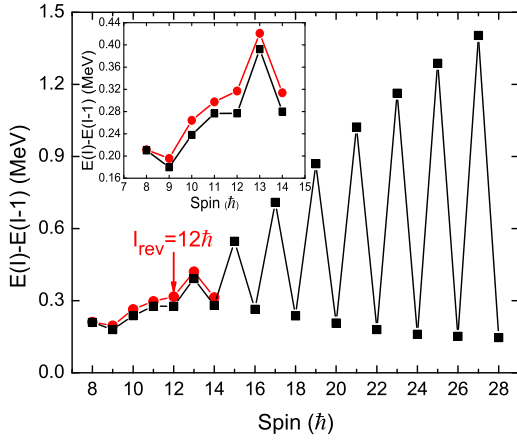


FIG. 7. (Color online) $E(I) - E(I - 1)$ vs spin for the yrast band of ^{114}Rh up to $28\hbar$. Experimental data are indicated in solid circles. Theoretical results based on the triaxially projected shell model are also shown in open squares. The arrow marks the reversion spin I_{rev} where the signature reversion occurs. The insert demonstrates the enlargement from $I = 8\hbar$ to $I = 14\hbar$.

σ in Eq. (1) specifies the states with the same angular momentum I . The two-body interaction Hamiltonian is then diagonalized in the projected basis. The mixing of the projected configurations is realized by the diagonalization, which describes fully quantum-mechanically the competition and possible transitions between different rotational modes.

The TPSM Hamiltonian consists of a set of separable forces

$$\hat{H} = \hat{H}_0 - \frac{1}{2}\chi \sum_{\mu} \hat{Q}_{\mu}^{\dagger} \hat{Q}_{\mu} - G_M \hat{P}^{\dagger} \hat{P} - G_Q \sum_{\mu} \hat{P}_{\mu}^{\dagger} \hat{P}_{\mu}. \quad (2)$$

In Eq. (2), \hat{H}_0 is the spherical single-particle Hamiltonian, which contains a proper spin-orbit force [31]. The second term is the quadrupole-quadrupole (QQ) interaction that includes the nn, pp, and np components.

The QQ interaction strength χ is determined in such a way that it has a self-consistent relation with the quadrupole deformation. The third term in Eq. (2) is the monopole pairing, whose strength G_M is of the simple standard form G/A with $G = 14.48$ MeV for neutrons and $G = 16.87$ MeV for protons used in the present work. The last term is the quadrupole pairing, with strength G_Q being proportional to G_M , $G_Q = 0.12G_M$. The triaxially deformed single-particle states for ^{114}Rh are generated by the Nilsson Hamiltonian with the deformation parameters $\varepsilon_2 = 0.253$ and $\gamma = 32^\circ$ (Lund convention), which are supported by Total Routhian Surface calculations. Three major shells, $N = 3, 4$, and 5 , are considered each for neutrons and protons.

The level energies $E(I)$ of the $\pi g_{9/2} \otimes \nu h_{11/2}$ yrast band in ^{114}Rh have been calculated up to $I = 28\hbar$, and the experimental level energies are well reproduced. In Fig. 7, the experimental $E(I) - E(I - 1)$, solid circles, are compared with the values calculated by the TPSM, open squares. From Fig. 7, it is seen that the signature splitting and the staggering behavior have been well reproduced, especially for the reversion spin $12\hbar$. The calculation predicts that the signature splitting increases with increasing spins after the reversion spin $I_{\text{rev}} = 12\hbar$. Unfortunately, such a behavior can not be well seen in experimental data due to the limits of highest spin measured. However, the tendency of the increasing signature splitting can be foreseen from the experimental data where the quantity $E(I) - E(I - 1)$ has a significantly enhanced staggering after $I = 12\hbar$, in comparison with those at lower spins, as shown in Fig. 7. The feature of the increasing signature splitting with the fast rotation characterizes the collective rotation, which will be discussed in more details next.

To probe the nature of the rotational motion of the triaxially shaped nucleus ^{114}Rh , calculations have been carried out for the expectation values of three components of the total angular momentum along the principal axes by using the TPSM wave functions from diagonalization that has reproduced the experimental data well,

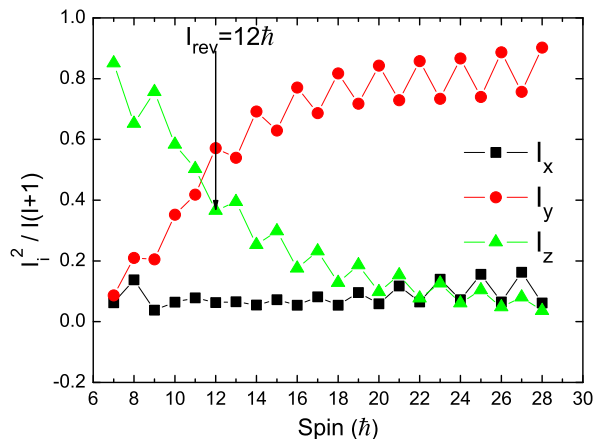


FIG. 8. (Color online) Calculated expectation values of I_x^2 , I_y^2 , and I_z^2 in unit of $I(I+1)$ with the wave functions from diagonalization that has reproduced the ^{114}Rh experimental data.

as seen in Fig. 7. The calculated $I_i^2/I(I+1)$, where $i = x, y$, and z , vs spin are plotted in Fig. 8.

The distinguishing feature of a crossing between the I_y^2 and I_z^2 curves around $12\hbar$, as shown in Fig. 8, indicates a change of the rotational mode. There exist two elementary modes of excitations for building the angular momentum in a highly rotating, deformed nucleus. The angular momentum may be due to the collective rotation around a principal axis or by means of the alignments of the angular momenta of the valence particles. In a triaxial nucleus, the alignments of the quasi-particles may occur along the shortest axis, called rotational alignment, or along the longest axis, called deformation alignment. The collective rotation in a superfluid triaxial nucleus proceeds along the principal axis of medium length, called principal axis rotation. At spins lower than $12\hbar$, the states of the $\pi g_{9/2} \otimes \nu h_{11/2}$ band in ^{114}Rh have deformation alignment, where I_z , the projection of the total angular momentum along the z -axis, is the largest. The large values of I_z are contributed by the alignments of the last neutron and the last proton along the z -axis because the neutron and proton Fermi levels lie at more than a half shell of the $h_{11/2}$ and the $g_{9/2}$ sub-shells, respectively. In contrast, at spins higher than $16\hbar$, the states behave as the collective rotation in which I_y dominates. It is interesting to see that the crossing between I_y and I_z occurs at around the experimental $I_{\text{rev}} = 12\hbar$. Therefore, it is a reasonable suggestion that the observed signature inversion be attributed to the change of the rotational mode, from the quasi-particle aligned rotation to the collective rotation along the intermediate principal axis. At low spins, the angular momentum is mainly built by the alignments of the last $h_{11/2}$ neutron and $g_{9/2}$ proton, while being in a competition with the strong

collective rotation, so the situation is somewhat complicated. At spins larger than $12\hbar$, the signature splitting has its normal phase and increases with increasing spins, as seen Fig. 7, and these are indeed the characteristics of the collective rotation, or principal axis rotation.

It is worth mentioning that the present work is the first investigation of signature inversion in neutron-rich $A \approx 110$ isotopes, which has opened up new challenges to both experiment and theory. This work extends the application of the triaxial projected shell model from the $A = 130$ region to the $A = 110$ region as the mechanism of signature inversion. Note that the studies in Ref. [29] indicate the impact of the residual proton-neutron interactions merely modifying the position of the reversion spin.

IV. CONCLUSION

The present work established a high-spin level scheme of ^{114}Rh for the first time by studying the γ -rays from the spontaneous fission of ^{252}Cf with Gammasphere. The level scheme bears a remarkable similarity to those of lighter odd-odd Rh isotopes. We assigned spins and parities to levels in the yrast band which has a configuration of $\pi g_{9/2} \otimes \nu h_{11/2}$. A side-band feeding the yrast 8^- state and a relatively large signature splitting in the yrast band indicate triaxiality playing a role in the structure of ^{114}Rh . The phenomenon of signature inversion was observed in the yrast band of ^{114}Rh with $I_{\text{rev}} = 12\hbar$. The triaxial projected shell model was used to interpret the signature inversion in ^{114}Rh . Model calculations successfully predicted $I_{\text{rev}} = 12\hbar$ and reproduced the experimental level energies in ^{114}Rh very well. Further examinations showed that the change of the rotational mode from quasi-particle aligned rotation to collective rotation along the intermediate axis of the triaxial ellipsoid can give rise to signature inversion in ^{114}Rh .

ACKNOWLEDGMENTS

The work at Vanderbilt University, UNIRIB/Oak Ridge Associated Universities, Mississippi State University, and Lawrence Berkeley National Laboratory is supported by the U.S. Department of Energy under Grant and Contract Nos. DE-FG05-88ER40407, DE-AC05-76OR00033, DE-FG02-95ER40939, and DE-AC03-76SF00098. The work at Tsinghua University and China Institute of Atomic Energy is supported by the National Natural Science Foundation of China under Grants Nos. 10775078, 11021504, and 10775182 and the Chinese Major State Basic Research Development Program through Grant No. 2007CB815005.

[1] H. Mach *et al.*, Phys. Lett. B **230**, 21 (1989).

[2] J. Skalski, S. Mizutori, and W. Nazarewicz, Nucl. Phys. **A617**, 282 (1997).

- [3] J. H. Hamilton *et al.*, Prog. Part. Nucl. Phys. **35**, 635 (1995).
- [4] A. G. Smith *et al.*, Phys. Rev. Lett. **77**, 1711 (1996).
- [5] H. Hua, *et al.*, Phys. Rev. C **69**, 014317 (2004).
- [6] Y. X. Luo *et al.*, Phys. Rev. C **70**, 044310 (2004); Y. X. Luo *et al.*, J. Phys. G: Nucl. Part. Phys. **31**, 1303 (2005); Y. X. Luo *et al.*, Phys. Rev. C **74**, 024308 (2006).
- [7] Y. X. Luo *et al.*, Phys. Rev. C **69**, 024315 (2004).
- [8] R. Duffait *et al.*, Nucl. Phys. **A454**, 143 (1986).
- [9] N. Fotiades *et al.*, Phys. Rev. C **67**, 064304 (2003) and references therein.
- [10] P. Joshi *et al.*, Phys. Lett. B **595**, 135 (2004).
- [11] <http://www.nndc.bnl.gov/ensdf/>
- [12] J. Timár *et al.*, Nucl. Phys. **A696**, 241 (2001).
- [13] J. Timár *et al.*, Acta Phys Pol B **33**, 493 (2002).
- [14] R. R. Zheng, S. Q. Zhu and X. D. Luo, Int. J. Mod. Phys. E **12**, 59 (2003).
- [15] R. R. Zheng *et al.*, Chin. Phys. Lett. **21**, 1475 (2004).
- [16] A. Jokinen *et al.*, Nucl. Phys. **A549**, 420 (1992).
- [17] G. Lhersonneau, Y. Wang, R. Capote, J. Suhonen, P. Dendooven, J. Huikari, K. Peräjärvi and J. C. Wang, Phys. Rev. C **67**, 024303 (2003).
- [18] D. C. Radford, Nucl. Instrum. Methods Phys. Res. A **361**, 297 (1995).
- [19] S. H. Liu, *et al.*, Phys. Rev. C **79**, 067303 (2009).
- [20] C. T. Zhang *et al.*, Phys. Rev. Lett. **77**, 3743 (1996).
- [21] W. B. Walters, E. A. Henry and R. A. Meyer, Phys. Rev. C **29**, 991 (1984).
- [22] P. Bhattacharyya *et al.*, Phys. Rev. C **56**, R2363 (1997).
- [23] S. H. Liu *et al.*, Phys. Rev. C **80**, 044314 (2009); S. H. Liu *et al.*, Phys. Rev. C **81**, 037302 (2010); S. H. Liu *et al.*, Phys. Rev. C **81**, 057304 (2010).
- [24] Y. X. Luo *et al.*, Nucl. Phys. **A838**, 1 (2010).
- [25] A. Bohr and B. R. Mottelson, *Nuclear Structure* (W. A. Benjamin, Inc., New York, 1975), Vol. II.
- [26] I. Hamamoto, Phys. Lett. B **235**, 221 (1990).
- [27] D. J. Hartley *et al.*, Phys. Rev. C **65**, 044329 (2002).
- [28] K. Hara and Y. Sun, Nucl. Phys. **A531**, (1991) 221.
- [29] Z. C. Gao, Y. S. Chen and Y. Sun, Phys. Lett. B **634**, 195 (2006).
- [30] A. Gelberg *et al.*, Nucl. Phys. **A557**, 439c (1993).
- [31] T. Bengtsson and I. Ragnarsson, Nucl. Phys. **A436**, 14 (1985) .